A Speed-Sensorless Predictive Current Control of Multiphase Induction Machines Using a Kalman Filter for Rotor Current Estimator

Magno Ayala*, Osvaldo Gonzalez*, Jorge Rodas*, Raul Gregor* and Jesus Doval-Gandoy†
*Laboratory of Power and Control Systems, Facultad de Ingeniería, Universidad Nacional de Asunción, Paraguay
E-mail: {mayala, ogonzalez, jrodas & rgregor}@ing.una.py
†Applied Power Electronics Technology Research Group, University of Vigo, Spain
E-mail: jdoval@uvigo.es

***Abstract*—In electrical drive applications based on induction machines, such as the propulsion drive of an electric vehicle, the rotor currents cannot be measured, so it needs to be estimated. This paper describes the rotor currents estimation through reduced order estimator known as Kalman filter to apply a speed-sensorless control of dual three-phase induction machines by applying a current inner loop based on the model predictive control. Simulation results are shown to demonstrate the efficiency of the proposed speed-sensorless control technique, thus concluding that the system can work properly without the speed sensor.**

***Index Terms*—Electric vehicle, multiphase machine, predictive control, sensorless control, Kalman filter.**

I. Introduction

In the last decade, the interest in multiphase machines has risen due to intrinsic features such as lower torque ripple, power splitting or better fault tolerance than three-phase machines. Recent research works and developments support the prospect of future more widespread applications of multiphase machines. In recent times, some of the applications of multiphase machines are being studied, such as electric vehicles (EV) and railway traction, all-electric ships, more-electric aircraft, and wind power generation systems [1].

EV is a road vehicle which requires an electric propulsion system. With this definition in mind, EVs may include battery electric vehicles, hybrid electric vehicles and fuelcell electric vehicles. The electric propulsion drive of an EV basically consists of a battery pack, an electronic power converter, an electric motor, and a speed and/or torque sensor. Considering multiphase machines as the electrical motor has several advantages, i.e. fault tolerance and higher power splitting across the different phases [2]. Due to the benefits of multiphase machines it can be applied in propulsion applications, like more electric aircraft [3], electrical and hybrid vehicles [4].

To be able to control the variables of the dual three-phase induction machines (DTPIM), the most used methods are the vector control using an inner loop current control and the direct torque control (DTC) [5]. However, DTC has some problems such as: weakness in torque control at very low speed, torque and flux pulsations due to the hysteresis bands in comparators, and variable frequency behavior [6]. On the other hand, field oriented control (FOC) or vector control has good current behavior, but it contains one speed control loop, four current control loops, one flux control loop and some transformation models for different coordinate frames. Thus, the complexity and cost of the control system is increased. But, compared to FOC, model predictive control (MPC) is more intuitive and easier to implement. For that matter, predictive current control (PCC) is an important line of Finite-State MPC. Currents are controlled with a notorious precision, while the system dynamic performance is also very good [7]. There are active research areas focused on the development of speed sensorless control algorithms due to their benefits compared to the conventional control techniques such as the elimination of the sensor wiring, better noise immunity, an increased reliability and less maintenance requirements [5]–[7].

Although speed sensorless operation of a three-phase induction machines is already well developed, little work has been conducted for multiphase induction machines [8]. Besides, some of the control loops on the MPC have unmeasured variables, such as rotor current, so a state observer is required [9]. The observers are mainly classified into two groups: deterministic observers such as Luenberger observer (LO) [5], model reference adaptive system (MRAS) [10], sliding mode observer (SMO) [11] and stochastic observer such as Kalman filter (KF) [9], being the KF the best choice to obtain high-accuracy estimates of dynamic system states [12].

This paper considers the sensorless speed control of DTPIM for EVs by using an inner loop of MPC, to predict the effects of future control decisions on the state-space variables. In order to accomplish this purpose, the proposed algorithm uses reduced order estimators based on a KF to estimate the rotor currents. After that, the estimated rotor currents are used to obtain an estimation of the mechanical speed of the machine. The efficiency of the proposed control technique in a DTPIM drive for varying load operations and varying speeds is studied .

This paper is organized as follows. Section II describes the DTPIM drive, Section III presents the mathematical model of the machine, Section IV details the predictive model with the speed observer and the current control with rotor current

978-1-5090-0813-1/16/$31.00 ©2016 IEEE

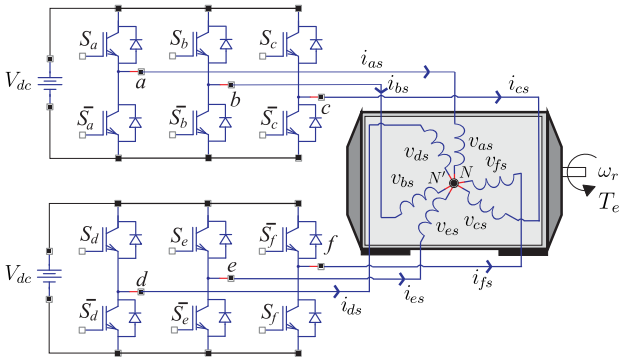

Fig. 1. A general scheme of a dual three-phase induction machine.

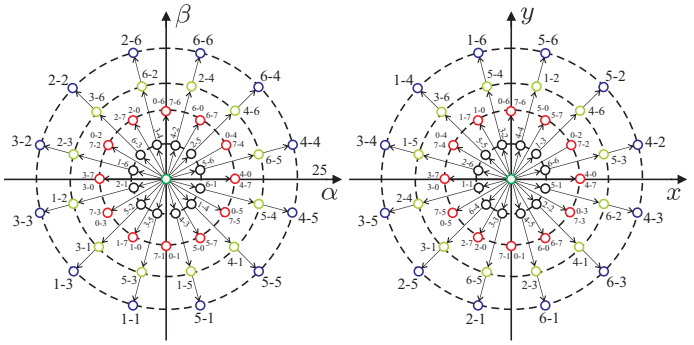

Fig. 2. Voltage space vectors and switching states in the $(\alpha-\beta)$ and $(x-y)$ subspaces for a dual three-phase VSI.

estimator based on KF and presents the proposed predictive control method for the dual three-phase induction machine. Simulation results are provided in Section V, showing the efficiency obtained by speed estimator. The conclusions are finally summarized in the last section.

II. The Dual Three-Phase Induction Machine Drive

The system under study consists of an DTPIM fed by a dual three-phase VSI and a dc link. A detailed scheme of the drive is provided in Fig. 1.

This DTPIM is a continuous system which can be analyzed by a group of differential equations. The system's model can be simplified through the vector space decomposition (VSD) firstly introduced in [13]. Thus, the original six-dimensional space of the machine is converted into three two-dimensional orthogonal subspaces in the stationary reference frame $(\alpha-\beta)$, $(x-y)$ and (z_1-z_2). This transformation is obtained through a 6 x 6 transformation matrix:

$$\mathbf{T}=\frac{1}{3}\begin{bmatrix} 1 & \frac{\sqrt{3}}{2} & -\frac{1}{2} & -\frac{\sqrt{3}}{2} & -\frac{1}{2} & 0 \\ 0 & \frac{1}{2} & \frac{\sqrt{3}}{2} & \frac{1}{2} & -\frac{\sqrt{3}}{2} & -1 \\ 1 & -\frac{\sqrt{3}}{2} & -\frac{1}{2} & \frac{\sqrt{3}}{2} & -\frac{1}{2} & 0 \\ 0 & \frac{1}{2} & -\frac{\sqrt{3}}{2} & \frac{1}{2} & \frac{\sqrt{3}}{2} & -1 \\ 1 & 0 & 1 & 0 & 1 & 0 \\ 0 & 1 & 0 & 1 & 0 & 1 \end{bmatrix} \tag{1}$$

where an amplitude invariant criterion was used.

For a machine with distributed windings, the $(\alpha-\beta)$ subspace contributes to useful power conversion (i.e. flux and torque production), while the $(x-y)$ and (z_1-z_2) components only result in losses and are usually minimized, except during post-fault operations. For two isolated neutrals configuration, both (z_1-z_2) currents cannot flow, so the (z_1-z_2) components can be ignored [14].

The voltage-source-inverter (VSI) has a discrete nature, actually, it has a total number of $2^6=64$ different switching states defined by six switching functions which are related to the six inverter legs $[S_a, S_b, S_c, S_d, S_e, S_f]$, where $\mathbf{S}_i \in \{0,1\}$. The finite switching states and the voltage of the DC link (Vdc) determine the phase voltages which can be mapped to the $(\alpha-\beta)-(x-y)$ space according to the VSD analysis. For this reason, the 64 on/off combinations of the six VSI legs lead to 64 space vectors in the $(\alpha-\beta)$ and $(x-y)$ subspaces. Fig. 2 shows the voltage space vectors in the $(\alpha-\beta)$ and $(x-y)$ subspaces, where each vector switching state is identified using the switching function by two octal numbers corresponding to the binary numbers $[S_aS_cS_e]$ and $[S_bS_dS_f]$, respectively.

As shown in Fig. 2 the 64 voltage vectors are reduced to only 49 different vectors in the $(\alpha-\beta)-(x-y)$ subspace. Moreover, a transformation matrix must be applied to convert the stationary reference frame $(\alpha-\beta)$ in the dynamic reference $(d-q)$. This matrix is given by:

$$\mathbf{T}_{dq}=\begin{bmatrix} cos\,(\delta_r) & -sin\,(\delta_r) \\ sin\,(\delta_r) & cos\,(\delta_r) \end{bmatrix} \tag{2}$$

where δ_r is the rotor angular position referred to the stator.

III. The Machine Modeling

It is feasible to model the machine by using an state-space representation, based on the VSD analysis and the dynamic reference conversion. This model is associated by:

$$\begin{aligned} \frac{d}{dt}\mathbf{X}_{\alpha\beta xy} &= \mathbf{A}\mathbf{X}_{\alpha\beta xy}+\mathbf{B}\mathbf{U}_{\alpha\beta xy} \\ \mathbf{Y}_{\alpha\beta xy} &= \mathbf{C}\mathbf{X}_{\alpha\beta \mathbf{xy}} \end{aligned} \tag{3}$$

where $\mathbf{U}_{\alpha\beta xy} = \begin{bmatrix} u_{\alpha s} & u_{\beta s} & u_{xs} & u_{ys} & 0 & 0 \end{bmatrix}^T$ stands for the input vector of the system, $\mathbf{X}_{\alpha\beta xy} = \begin{bmatrix} i_{\alpha s} & i_{\beta s} & i_{xs} & i_{ys} & i_{\alpha r} & i_{\beta r} \end{bmatrix}^T$ denotes the state vector, $\mathbf{Y}_{\alpha\beta xy} = \begin{bmatrix} i_{\alpha s} & i_{\beta s} & i_{xs} & i_{ys} & 0 & 0 \end{bmatrix}^T$ indicates the output vector and $\mathbf{A}$, $\mathbf{B}$ and $\mathbf{C}$ are matrices that define the dynamics of the electrical drive.

The mechanical section of the electrical drive is defined by the following equations:

$$T_e = 3P\left(\psi_{\alpha s}i_{\beta s}-\psi_{\beta s}i_{\alpha s}\right) \tag{4}$$

$$J_i\frac{d}{dt}\omega_r + B_i\omega_r = P\left(T_e-T_L\right) \tag{5}$$

where ω_r is the rotor angular speed, T_e is the generated torque, T_L denotes the load torque, B_i the friction coefficient, $\psi_{\alpha s}$ and $\psi_{\beta s}$ the stator fluxes, J_i the inertia coefficient and P the number of pairs of poles.

IV. Proposed predictive model

By considering the mathematical model expressed by (3) and using the state-space variables defined by the vector $\mathbf{X}_{\alpha\beta xy}$, we can determine the following group of equations:

$$\begin{aligned}
\frac{d}{dt}(x_1) &= -R_s c_2 x_1 + c_4 (L_m \omega_r x_2 + R_r x_5 + L_r \omega_r x_6) \\
&\quad + c_2 u_1 \\
\frac{d}{dt}(x_2) &= -R_s c_2 x_2 + c_4 (-L_m \omega_r x_1 - L_r \omega_r x_5 + R_r x_6) \\
&\quad + c_2 u_2 \\
\frac{d}{dt}(x_3) &= -R_s c_3 x_3 + c_3 u_3 \\
\frac{d}{dt}(x_4) &= -R_s c_3 x_4 + c_3 u_4 \\
\frac{d}{dt}(x_5) &= -R_s c_4 x_1 + c_5 (-L_m \omega_r x_2 - R_r x_5 - L_r \omega_r x_6) \\
&\quad - c_4 u_1 \\
\frac{d}{dt}(x_6) &= -R_s c_4 x_2 + c_5 (L_m \omega_r x_1 + L_r \omega_r x_5 - R_r x_6) \\
&\quad - c_4 u_2
\end{aligned} \tag{6}$$

where R_s, R_r, L_m, $L_s = L_{ls} + L_m$ and $L_r = L_{lr} + L_m$ are the electrical parameters of the DTPIM and the coefficients c_i for $i = 1, \ldots, 5$, are defined as $c_1 = L_s L_r - L_m^2$, $c_2 = \frac{L_r}{c_1}$, $c_3 = \frac{1}{L_{ls}}$, $c_4 = \frac{L_m}{c_1}$ and $c_5 = \frac{L_s}{c_1}$, while the input vector corresponds to the voltages applied to the stator $u_1 = v_{\alpha s}$, $u_2 = v_{\beta s}$, $u_3 = v_{xs}$, $u_4 = v_{ys}$ and the state vector corresponds to the DPTIM currents $x_1 = i_{\alpha s}$, $x_2 = i_{\beta s}$, $x_3 = i_{xs}$, $x_4 = i_{ys}$, $x_5 = i_{\alpha r}$ and $x_6 = i_{\beta r}$.

Stator voltages are defined from the input control signals by means of the inverter model. So, the simplest model, used for isolated neutral configuration, has been considered in order to obtain a fast optimization process. Given that the gating signals are arranged in the vector $\mathbf{S} = [S_a, S_b, S_c, S_d, S_e, S_f]$, we can obtain the stator voltages from:

$$\mathbf{M} = \frac{1}{3} \begin{bmatrix} 2 & 0 & -1 & 0 & -1 & 0 \\ 0 & 2 & 0 & -1 & 0 & -1 \\ -1 & 0 & 2 & 0 & -1 & 0 \\ 0 & -1 & 0 & 2 & 0 & -1 \\ -1 & 0 & -1 & 0 & 2 & 0 \\ 0 & -1 & 0 & -1 & 0 & 2 \end{bmatrix} \cdot \mathbf{S}^T \tag{7}$$

An ideal inverter converts gating signals into stator voltages which are projected to $(\alpha - \beta)$ and $(x - y)$ subspaces and joined in a row vector $\mathbf{U}_{\alpha\beta xy}$ defined as:

$$\mathbf{U}_{\alpha\beta xy} = [u_{\alpha s} \;\; u_{\beta s} \;\; u_{xs} \;\; u_{ys} \;\; 0 \;\; 0]^T = Vdc \cdot \mathbf{M} \cdot \mathbf{T} \tag{8}$$

where Vdc is the dc link voltage and the superscript $(^T)$ indicates a transposed matrix. By using the rotational transformation (2) to the $(\alpha - \beta)$ components, we get:

$$\mathbf{U}_{dq} = [u_{ds} \, u_{qs}]^T = \mathbf{T}_{dq} \cdot \begin{bmatrix} u_{\alpha s} \\ u_{\beta s} \end{bmatrix} \tag{9}$$

By gathering the equations (6)-(9) a nonlinear group of equations appears which can be spelled in the state space representation:

$$\begin{aligned}
\dot{\mathbf{X}}_{(t)} &= f\left(\mathbf{X}_{(t)}, \, \mathbf{U}_{(t)}\right) \\
\mathbf{Y}_{(t)} &= \mathbf{C}\mathbf{X}_{(t)}
\end{aligned} \tag{10}$$

where the state vector is defined as $\mathbf{X}_{(t)} = [x_1, \, x_2, \, x_3, \, x_4, x_5, \, x_6]^T$, the input vector as $\mathbf{U}_{(t)} = [u_1, \, u_2, u_3, \, u_4]$, and $\mathbf{Y}_{(t)} = [x_1, \, x_2, x_3, \, x_4]^T$ as the output vector. The parts of the vectorial function f and the matrix $\mathbf{C}$ are obtained through a straightforward way from (6) and the state and output vector definitions. The model (10) needs to be discretized so it can be used by the predictive controller. A forward Euler method is selected to maintain a low computational cost. For this reason, the obtained equations will have the required digital control form, with predicted variables depending only on the past values and not on present ones of the variables. So, a prediction of the next-sample state $\hat{\mathbf{X}}_{[k+1|k]}$ can be expressed as:

$$\hat{\mathbf{X}}_{[k+1|k]} = \mathbf{X}_{[k]} + T_m f\left(\mathbf{X}_{[k]}, \, \mathbf{U}_{[k]}, \, \omega_{r[k]}\right) \tag{11}$$

where T_m is the sampling time and $[k]$ is the present sample.

A. Reduced order estimators

In the state space representation (10), only the stator voltages, currents and the mechanical speed can be measured. The stator voltages are very easy to predict from the switching commands generated from the VSI. However, the rotor currents cannot be directly measured. This predicament can be surpassed through the estimation of the rotor currents by using the reduced order estimators. The reduced order estimators prepare an estimation for only the unmeasured portion of the state vector, so, the evolution of states can be spelled as:

$$\begin{aligned}
\underbrace{\begin{bmatrix} \hat{\mathbf{X}}_{a[k+1|k]} \\ \hat{\mathbf{X}}_{b[k+1|k]} \\ \hat{\mathbf{X}}_{c[k+1|k]} \end{bmatrix}}_{[\hat{\mathbf{X}}_{[k+1|k]}]} &= \underbrace{\begin{bmatrix} \overline{\mathbf{A}}_{11} & \overline{\mathbf{A}}_{12} & \overline{\mathbf{A}}_{13} \\ \overline{\mathbf{A}}_{21} & \overline{\mathbf{A}}_{22} & \overline{\mathbf{A}}_{23} \\ \overline{\mathbf{A}}_{31} & \overline{\mathbf{A}}_{32} & \overline{\mathbf{A}}_{33} \end{bmatrix}}_{[\mathbf{A}]} \underbrace{\begin{bmatrix} \mathbf{X}_{a[k]} \\ \mathbf{X}_{b[k]} \\ \mathbf{X}_{c[k]} \end{bmatrix}}_{[\mathbf{X}_{[k]}]} \\
&\quad + \underbrace{\begin{bmatrix} \overline{\mathbf{B}}_1 \\ \overline{\mathbf{B}}_2 \\ \overline{\mathbf{B}}_3 \end{bmatrix}^T}_{[\mathbf{B}]} \underbrace{\begin{bmatrix} \mathbf{U}_{\alpha\beta s} \\ \mathbf{U}_{xys} \\ \mathbf{U}_{\alpha\beta s} \end{bmatrix}}_{[\mathbf{U}_k]}
\end{aligned} \tag{12}$$

$$\mathbf{Y}_{[k]} = \underbrace{\begin{bmatrix} \overline{\mathbf{I}} & \overline{\mathbf{I}} & \overline{\mathbf{0}} \end{bmatrix}}_{[\mathbf{C}]} \underbrace{\begin{bmatrix} \mathbf{X}_{a[k]} \\ \mathbf{X}_{b[k]} \\ \mathbf{X}_{c[k]} \end{bmatrix}}_{[\mathbf{X}_{[k]}]} \tag{13}$$

where $\mathbf{X}_a = [i_{\alpha s} i_{\beta s}]^T$, $\mathbf{X}_b = [i_{xs} i_{ys}]^T$, $\mathbf{X}_c = [i_{\alpha r} i_{\beta r}]^T$, $\mathbf{U}_{\alpha\beta s} = [U_{\alpha s} U_{\beta s}]^T$, $\mathbf{U}_{xys} = [U_{xs} U_{ys}]^T$, $\mathbf{A}$ and $\mathbf{B}$ are matrices which are dependent on the electrical parameters of the DTPIM and the sampling time T_m. Matrix [A] is also dependable on the present value of $\omega_{r[k]}$, which is calculated every sampling time [9].

B. Rotor current estimation based on Kalman filters

The KF design considers uncorrelated process and zero-mean Gaussian measurement noises, so the systems equations can be defined as:

$$\hat{\mathbf{X}}_{[k+1]} = \mathbf{A}\mathbf{X}_{[k]} + \mathbf{B}\mathbf{U}_{[k]} + \mathbf{H}\varpi_{[k]} \tag{14}$$

$$\mathbf{Y}_{[k+1]} = \mathbf{C}\mathbf{X}_{[k+1]} + \nu_{[k+1]} \tag{15}$$

being $\nu_{[k+1]}$ the measurement noise, $\mathbf{H}$ the noise weight matrix and $\varpi_{[k]}$ the process noise.

The dynamics of the KF can be written as follows:

$$\begin{aligned}\hat{\mathbf{X}}_{c[k+1|k]} = (\mathbf{A}_{33} - \mathbf{K}_{[k]}\mathbf{A}_{13})\hat{\mathbf{X}}_{c[k]} + \mathbf{K}_{[k]}\mathbf{Y}_{[k+1]} + \\ (\mathbf{A}_{31} - \mathbf{K}_{[k]}\mathbf{A}_{11})\mathbf{Y}_{[k]} + (\mathbf{B}_3 - \mathbf{K}_{[k]}\mathbf{B}_1)\mathbf{U}_{\alpha\beta s[k]}\end{aligned} \tag{16}$$

where $\mathbf{K}_{[k]}$ is the KF gain matrix which is obtained from the covariances of the process and measurement noises for each sampling time in a recursive manner as:

$$\mathbf{K}_{[k]} = \mathbf{\Gamma}_{[k]} \cdot \mathbf{C}^T \widehat{R}_\nu^{-1} \tag{17}$$

where $\mathbf{\Gamma}_{[k]}$ is the covariance of the new estimation, that it's determined as a function of the old covariance estimation ($\varphi_{[k]}$) as shown:

$$\mathbf{\Gamma}_{[k]} = \varphi_{[k]} - \varphi_{[k]} \cdot \mathbf{C}^T (\mathbf{C} \cdot \varphi_{[k]} \cdot \mathbf{C}^T + \widehat{R}_\nu)^{-1} \cdot \mathbf{C} \cdot \varphi_{[k]} \tag{18}$$

From the state space equation, that includes the process noise, it's possible to obtain a correction of the estimated state covariance as follows:

$$\varphi_{[k+1]} = \mathbf{A}\mathbf{\Gamma}_{[k]} \cdot \mathbf{A}^T + \mathbf{H}\widehat{Q}_\varpi \cdot \mathbf{H}^T \tag{19}$$

These equations are the required relations in order to get the optimal state estimation using KF with PCC. So, $\mathbf{K}_{[k]}$ provides minimum estimation errors, by knowing the measurement noise magnitude ($\widehat{R}_\nu$), the process noise magnitude ($\widehat{Q}_\varpi$) and ($\varphi_{[0]}$) being the covariance initial condition.

This design of the KF, in terms of a robust covariance estimation, isn't the goal of our work, that is mainly set in a concept analysis of the speed sensorless technique. In our case, the KF gains will be adjusted based on a heuristic method. After all, it can be assumed that the estimated rotor states will provide sub-optimal results, which could get better by using more proper KF design methods.

C. The speed observer

After obtaining the unmeasurable rotor state values, the speed can be calculated from the dynamic equation which defines the mechanical section of the electrical drive (4) and (5) by using the Euler forward method. So the estimated speed can be obtained from the discrete equation which follows:

$$\hat{\omega}_{r[k+1]} = \frac{T_m P}{J_i}(T_{e[k]} - T_{L[k]}) + (1 - \frac{T_m B_i}{J_i})\hat{\omega}_{r[k]} \tag{20}$$

where it's taken $\omega_{r[0]} = 0$, $T_{L[0]} = 0$ and the unmeasured rotor states $i_{\alpha\beta r[0]} = 0$.

D. Cost function

The cost function must include all the terms which have to be optimized. In PCC the most important term is the tracking error generated in the predicted stator currents for the next sample. In order to minimize its error in each sample k it's necessary to apply a simple equation such as:

$$\begin{aligned}J_{[k+2|k]} =& \hat{e}_{i\alpha s[k+2]} + \hat{e}_{i\beta s[k+2]} + \lambda_{xy}\left(\hat{e}_{ixs[k+2]} + \hat{e}_{iys[k+2]}\right) \\ \hat{e}_{i\alpha s[k+2]} =& \parallel i^*_{\alpha s[k+2]} - \hat{i}_{\alpha s[k+2]} \parallel^2 \\ \hat{e}_{i\beta s[k+2]} =& \parallel i^*_{\beta s[k+2]} - \hat{i}_{\beta s[k+2]} \parallel^2 \\ \hat{e}_{ixs[k+2]} =& \parallel i^*_{xs[k+2]} - \hat{i}_{xs[k+2]} \parallel^2 \\ \hat{e}_{iys[k+2]} =& \parallel i^*_{ys[k+2]} - \hat{i}_{ys[k+2]} \parallel^2\end{aligned} \tag{21}$$

where $\parallel . \parallel$ represents the vector magnitude, $i^*_{s[k+2]}$ is a vector which contains the stator currents references and $\hat{i}_{s[k+2]}$ is a vector that defines the based predictions on the next state (including the delay compensation and control effort). More complex cost functions can be arranged to reduce the VSI losses and/or the harmonic distortion [12]–[15].

E. The optimizer

The proposed predictive model needs to include all 64 possibilities run to consider all possible voltage vectors. But, in Fig. 2 shows the redundancy of the switching space vectors by showing only 49 different vectors (48 active and 1 null). This consideration is commonly considered as the optimal solution. Now, for a generic multiphase machine, where g is the phase number and ε is the search vector space (49 for the DTPIM), the proposed optimization algorithm generates the optimal switching signal set $\mathbf{S}^{opt}$, and it's shown as follows:

Algorithm 1 Proposed optimization algorithm

1. **comment:** Algorithm initial values.
2. $J_o := \infty$, $i := 1$
3. **while** $i \leq \varepsilon$ **do**
4. $\quad \mathbf{S}_i \leftarrow \mathbf{S}_{i,j}\ \forall\, j = 1, ..., g$
5. $\quad$ **comment:** Stator voltages calculation. Eqn. 8.
6. $\quad U_{\alpha\beta xys} = [u_{\alpha s}\, u_{\beta s}\, u_{xs}\, u_{ys}\, 0\, 0]^T = Vdc \cdot \mathbf{M} \cdot \mathbf{T}$
7. $\quad$ **comment:** Calculate the prediction of the measurement stator current states, considering $\mathbf{X}_{b[0]} = 0$.
8. $\quad \mathbf{X}_{a[k+1]} = \overline{\mathbf{A}}_{11}\mathbf{X}_{a[k]} + \overline{\mathbf{B}}_1\mathbf{U}_{\alpha\beta s} + \overline{\mathbf{A}}_{12}\mathbf{X}_{b[k]}$
9. $\quad$ **comment:** Minimize the cost function. Eqn. 21.
10. $\quad J_{[k+2|k]} = \hat{e}_{i\alpha s[k+2]} + \hat{e}_{i\beta s[k+2]} + \lambda_{xy}\left(\hat{e}_{ixs[k+2]} + \hat{e}_{iys[k+2]}\right)$
11. $\quad$ **if** $J < J_o$ **then**
12. $\quad\quad J_o \leftarrow J$, $\mathbf{S}^{opt} \leftarrow \mathbf{S}_i$
13. $\quad$ **end if**
14. $\quad i := i + 1$
15. **end while**
16. **comment:** Calculate the prediction of the unmeasurable rotor current states. Eqn. 16.
17. $\hat{\mathbf{X}}_{b[k+1|k]} = (\mathbf{A}_{22} - \mathbf{K}_{[k]}\mathbf{A}_{12})\hat{\mathbf{X}}_{b[k]} + \mathbf{K}_{[k]}\mathbf{Y}_{[k+1]} + (\mathbf{A}_{21} - \mathbf{K}_{[k]}\mathbf{A}_{11})\mathbf{Y}_{[k]} + (\mathbf{B}_2 - \mathbf{K}_{[k]}\mathbf{B}_1)\mathbf{U}_{\alpha\beta s[k]}$

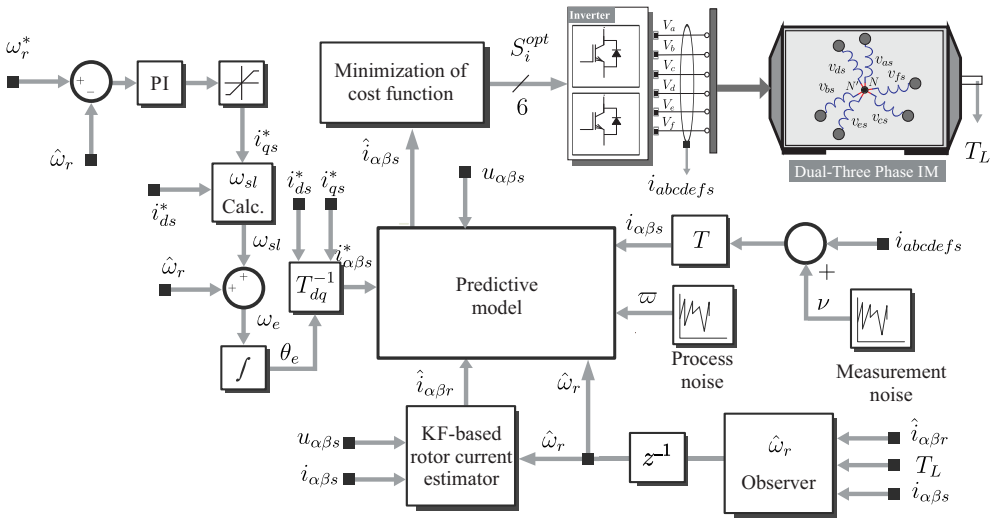

Fig. 3. Block diagram of the proposed speed sensorless control method for the DTPIM.

F. Proposed predictive current control technique

By analyzing the inner loop of the current predictive control, we consider a conventional predictive control which avoids the use of lineal controllers such as proportional-integer (PI) controllers and modulation methods since a single switching vector is selected during the whole switching period. This process is similar to original DTC techniques and ends having a variable switching frequency. The proposed predictive control method executes the control actions by solving an optimization problem for every sample time. A mathematical model of the real system, which is the DTPIM, is used to estimate its output. This estimation is accomplished for every possible output, or switching voltage vector, of the six-phase VSI to detect which one reduces a pre-selected cost function, and thus, the model of the DTPIM, also named as predictive model, must be used by considering all the 49 possible voltage vectors in the six-phase VSI. But since the rotor currents can not be measured directly, it need to be calculated by using a KF. The absolute stator current error, in the $(\alpha - \beta)$ subspace for the next sampling time, is currently used for computational cost reduction. For this case, the cost function $J_{[k+2|k]}$ is determined as (21), where $i^*_{\alpha s[k+1]}$ and $i^*_{\beta s[k+1]}$ are the stator reference currents and $i_{\alpha s[k+2}$ and $i_{\beta[k+2]}$ are the predicted stator currents that are computationally calculated by using the predictive model. A proportional integral (PI) controller with a saturator is selected for the speed sensorless control loop, which consists on the indirect vector control method because of its simplicity. In the indirect vector control method, the PI speed controller is used to obtain the dynamic reference current i^*_{qs}. The current reference, used by the proposed predictive model, are generated from the electric angle estimation used to transform the current reference, originally in the dynamic reference frame $(d-q)$, to the $(\alpha - \beta)$ subspace. The estimation process of the slip frequency (ω_{sl}) is executed in the same way as the Indirect Field Orientation techniques, from the electrical parameters of the DTPIM (L_r, R_r) and the reference currents in the dynamic reference frame (i^*_{ds}, i^*_{qs}). Finally, using the rotor current estimated, the stator current measured and the load torque measured from the induction machine we can estimate the speed of the machine. A block diagram of the proposed speed sensorless control method for the DTPIM electrical drive is shown in Fig. 3.

TABLE I
MECHANICAL AND ELECTRICAL PARAMETERS OF THE DTPIM

PARAMETER	SYMBOL	VALUE	UNIT
Rotor resistance	R_r	0.63	Ω
Stator resistance	R_s	0.62	Ω
Magnetizing inductance	L_m	199.8	mH
Rotor inductance	L_r	203.3	mH
Stator leakage inductance	L_{ls}	6.4	mH
Stator inductance	L_s	206.2	mH
Pairs of poles	P	3	–
System inertia	J_i	0.27	kg.m^2
Friction coefficient	B_i	0.012	kg.m^2/s
Nominal frequency	f_a	50	Hz
Electrical power	P_w	15	kW

V. SIMULATION RESULTS

A MATLAB/Simulink simulation program has been designed for the VSI connected to the DTPIM, and results have shown the efficiency of the proposed speed sensorless predictive control algorithm. A numerical integration defined by the first order Euler's discretization method has been selected to compute the prediction of the state space variables for every sample in the time domain. Table I shows the mechanical and electrical parameters for the DTPIM.

The efficiency of the proposed speed sensorless predictive control technique for the DTPIM has been tested, under load torque conditions. For every case, it's selected a sampling frequency of 10 kHz. In Fig. 4 we show the obtained results for a variable speed reference [180, 220, -220, -180] rpm,

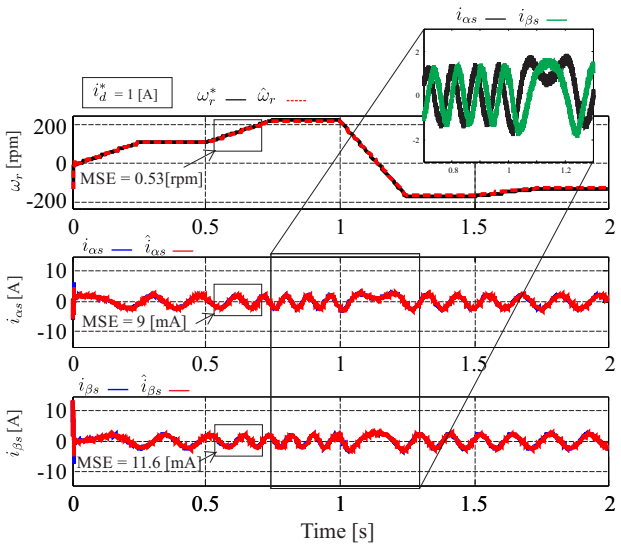

Fig. 4. Simulation results for a variable speed reference condition.

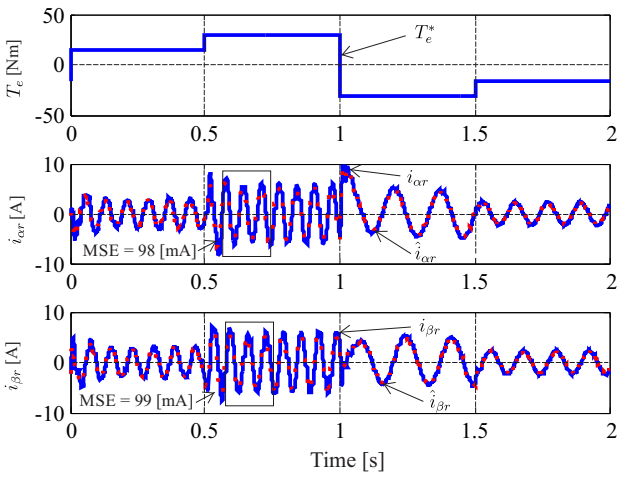

Fig. 5. Simulation results for a variable load torque condition.

considering a fixed dynamic reference current ($i_{ds}^* = 1$ A). The subscripts $(\alpha - \beta)$ represent the values in the $(\alpha - \beta)$ subspace regarding the stator currents. The calculated speed is fedback into the closed loop which is regulated by a PI controller as shown in Fig. 3. Besides, it can be appreciated from Fig. 4 (zoom), the phases changing by the stator currents in the $(\alpha - \beta)$ subspace, caused by the rotation of the DTPIM being reversed. Under these conditions, the mean squared error (MSE) in the current tracking and speed are 9 mA, 11.6 mA and 0.53 rpm, respectively.

In Fig. 5 is demonstrated a variable load torque condition response [15, 30, -30, -15] N·m, and the rotor currents evolution (measured and estimated) in the $(\alpha - \beta)$ subspace. In this figure, we can see the amplitude behavior of the rotor currents varying because of the load torque T_L applied to the DTPIM. The observed rotor currents values are very close to real values in these test conditions, considering that the MSE is 98 mA and 99 mA for $i_{\alpha r}$ and $i_{\beta r}$, respectively.

VI. Conclusion

In this paper, the electrical propulsion drive of EVs based in a sensorless speed control method of a DTPIM using an current inner loop based on the MPC technique is proposed. The MPC is designed through a state-space representation, where the stator and rotor currents are defined as state space variables. The rotor currents are calculated by using a KF. The theoretical analysis of the controller has been verified through simulation results. The technique prevents the use of a speed sensor and has shown its efficiency even when considering that the DTPIM is being operated under different speeds and load torque values.

Acknowledgment

The authors would like to give thanks to the Paraguayan Government for the economical support provided through a CONACYT grant project 14-INV-101.

References

[1] M. J. Duran and F. Barrero, "Recent advances in the design, modeling, and control of multiphase machines: Part: I," *IEEE Trans. Ind. Electron.*, vol. 63, no. 1, pp. 459–468, 2016.

[2] J. Riveros, B. Bogado, J. Prieto, F. Barrero, S. Toral, and M. Jones, "Multiphase machines in propulsion drives of electric vehicles," in *Proc. EPE/PEMC*, 2010, pp. T5–201.

[3] M. Villani, M. Tursini, G. Fabri, and L. Castellini, "High reliability permanent magnet brushless motor drive for aircraft application," *IEEE Trans. Ind. Electron.*, vol. 59, no. 5, pp. 2073–2081, 2012.

[4] L. Jin, S. Norrga, H. Zhang, and O. Wallmark, "Evaluation of a multiphase drive system in ev and hev applications," in *Proc. IEMDC*. IEEE, 2015, pp. 941–945.

[5] R. Gregor and J. Rodas, "Speed sensorless control of dual three-phase induction machine based on a luenberger observer for rotor current estimation," in *Proc. IECON*, 2012, pp. 3653–3658.

[6] A. Taheri and M. Mohammadbeigi, "Speed sensor-less estimation and predictive control of six-phase induction motor using extended kalman filter," in *Proc. PEDSTC*, 2014, pp. 13–18.

[7] F. Wang, X. Mei, H. Dai, S. Yu, and P. He, "Sensorless finite control set predictive current control for an induction machine," in *Proc. ICIA*, 2015, pp. 3106–3111.

[8] A. S. Morsy, A. Abdel-Khalik, S. Ahmed, and A. Massoud, "Sensorless field oriented control of five-phase induction machine under open-circuit phase faults," in *Proc. ECCE*, 2013, pp. 5112–5117.

[9] J. Rodas, F. Barrero, M. R. Arahal, C. Martin, and R. Gregor, "On-line estimation of rotor variables in predictive current controllers: A case study using five-phase induction machines," 2016.

[10] L. Zhao, J. Huang, H. Liu, B. Li, and W. Kong, "Second-order sliding-mode observer with online parameter identification for sensorless induction motor drives," *IEEE Trans. Ind. Electron.*, vol. 61, no. 10, pp. 5280–5289, 2014.

[11] M. Comanescu, "Design and implementation of a highly robust sensorless sliding mode observer for the flux magnitude of the induction motor," *IEEE Trans. Energy Convers.*, vol. 31, no. 2, pp. 649–657, 2016.

[12] R. Gregor, J. Rodas, J. Munoz, M. Ayala, O. Gonzalez, and D. Gregor, "Predictive-fixed switching frequency technique for 5-phase induction motor drives," in *Proc. SPEEDAM*, 2016.

[13] Y. Zhao and T. A. Lipo, "Space vector PWM control of dual three-phase induction machine using vector space decomposition," *IEEE Trans. Ind. Electron.*, vol. 31, no. 5, pp. 1100–1109, 1995.

[14] H. S. Che and W. P. Hew, "Dual three-phase operation of single neutral symmetrical six-phase machine for improved performance," in *Proc. IECON*, 2015, pp. 001 176–001 181.

[15] S. Kwak and S.-k. Mun, "Model predictive control methods to reduce common-mode voltage for three-phase voltage source inverters," *IEEE Trans. Ind. Electron.*, vol. 30, no. 9, pp. 5019–5035, 2015.